Numerical Simulation of Long-Term Climate Change in East Asia *

TANG Jianping (汤剑平), SU Bingkai (苏炳凯), ZHAO Ming (赵 鸣), and ZHAO Deming (赵得明)

Department of Atmospheric Sciences, Key Lab for Mesoscale Severe Weather of Education Ministry, Nanjing University, Nanjing 210093

(Received January 4, 2006)

ABSTRACT

A 10-yr regional climate simulation was performed using the fifth-generation PSU/NCAR Mesoscale Model Version 3 (MM5V3) driven by large-scale NCEP/NCAR reanalyses. Simulations of winter and summer mean regional climate features were examined against observations. The results showed that the model could well simulate the 10-yr winter and summer mean circulation, temperature, and moisture transport at middle and low levels. The simulated winter and summer mean sea level pressure agreed with the NCAR/NCEP reanalysis data. The model could well simulate the distribution and intensity of winter mean precipitation rates as well as the distribution of summer mean precipitation rates, but it overestimated the summer mean precipitation over North China. The model's ability to simulate the regional climate change in winter was superior to that in summer. In addition, the model could simulate the inter-annual variation of seasonal precipitation and surface air temperature. Geopotential heights and temperature at middle and high levels between simulations and observations exhibited high anomaly correlation coefficients. The model also showed large variability to simulate the regional climate change associated with the El Niño events. The MM5V3 well simulated the anomalies of summer mean precipitation in 1992 and 1995, while it demonstrated much less ability to simulate that in 1998. Generally speaking, the MM5V3 is capable of simulating the regional climate change, and could be used for long-term regional climate simulation.

Key words: East Asia, climate change, numerical simulation, MM5V3

1. Introduction

Recent studies on regional climate change simulations have shown that the regional climate model (RCM) has the potential ability to simulate and forecast the feature of regional climate change. The prevalent regional model is NCAR RegCM2 (Giorgi et al., 1993a, b) at present. With the development of mesoscale model, it has become probable to establish regional climate model based on the new generation mesoscale model. Many researchers have performed the regional climate simulation using the improved RCM based on the PSU/NCAR Mesoscale Model (MM5) (Jiang et al., 2002; Crawford et al., 2001; Wei et al., 2002; Xiong, 2001), and shown good results. Currently, the NCAR mesoscale model has evolved to MM5V3, which is non-hydrostatic, including the radiation and land-surface processes that are important for regional climate simulation, and developing detailed cumulus parameterization and boundary layer parameterization as well as the advanced treatment of initial and lateral boundary conditions. Because of these advancements, the model can be used for long-term regional climate simulation. Many regional climate simulation experiments have been implemented by using the MM5V3 model (Liang et al., 2001; Liu, 2003; Leung et al., 2003a, b).

East Asia is marked by unique topography, vegetation, and monsoon climate, and has relatively large climate variability in the world. The Tibetan Plateau situates in the west, the West Pacific Ocean in the east, complex topography and vegetation in the north, and the equatorial oceans in the south. The variation of regional monsoon climate in East Asia has significant impacts on the economic development directly. Therefore, understanding the mechanism of East Asian climate and research on regional monsoon climate plays an important role in Chinese national economy over this region. Since the 1990s the RCM was first introduced into China, the model has been used to perform many simulations in East Asia, but mostly with the emphasis on season-scale (Luo and Zhao, 1997;

*Supported by National Key Program for Developing Basic Sciences (G1999043400).

Zhao and Luo, 1998, 1999; Shi et al., 2001; Luo et al., 2002; Liu et al., 1996; Wang et al., 2002; Liu and Ding, 2001). For example, Chen and Fu (2000) implemented the regional climate model RegCM2 nested to the Australian global circulation model CSIRO to perform a 3-yr simulation. The results indicated that the RCM simulated better regional climate features than that by the global model compared with observations. Lee and Suh (2000) simulated the 10-yr East Asian climate change in summer using the NCAR RegCM2 and found that the model could represent the large scale features associated with East Asian summer monsoon. Of those simulations, however, some were performed on short-time scales or small regions. In order to examine the performance of each regional climate model in East Asia, Fu Chongbin organized Regional Model Intercomparison Plan (RMIP) over East Asia, which includes the second step of this plan to perform a 10-yr regional climate simulation in East Asia, with the region covering nearly all East Asia. As a portion of the RMIP work, the MM5V3 was used to simulate the 10-yr climate change in East Asia, and the preliminary results were analyzed in this paper.

2. Model and data

This study used the PSU/NCAR fifth generation mesoscale model MM5V3 (Dudhia et al., 2001), which was upgraded based on the MM4 and MM5V2. It is a nonhydrostatic model, coupling with the OSU land surface model (Chen and Dudhia, 2001a, b). The MM5V3 model has the fundamental capability to simulate regional climate change.

The model domain contains 111×151 grid points and is centered at 35°N, 110°E over China, covering most part of East Asia (Fig.1). The horizontal resolution is 60 km. The main physical parameterization schemes include Grell cumulus parameterization scheme, RRTM longwave radiation parameterization, Dudhia shortwave radiation parameterization, MRF boundary layer parameterization scheme, and OSU land surface process. The initial and lateral boundary conditions come from the NCAR/NCEP reanalysis data (Kalnay et al., 1996), which is at 2.5°×2.5° horizontal resolution with 16 sigma levels and a 6-h interval. The data are bilinearly interpolated into the model domain as initial and lateral boundary conditions. The top level in the model is at 100 hPa, while 15-grid buffer zones are on each side. The simulation periods are from 1 July 1988 to 1 January 1999 with an integration time step of 180 s. The integration is performed on the "Blue Light" high performance computer at Global Change Research Center of Nanjing University (Su et al., 2002).

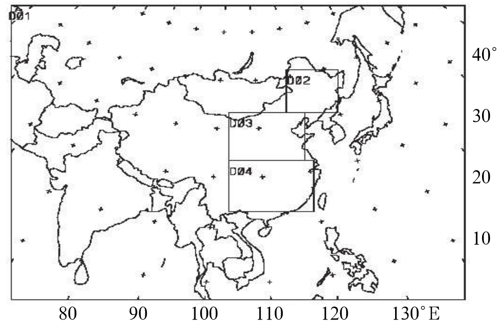

Fig.1. Simulation domain and three subdomains (D02: Northeast China, D03: North China, and D04: South China).

3. Model results

We analyzed the model results from January 1989 to December 1998, considering the first half year as the model spin-up time. The domain for analysis covers the most part of East Asia after removing the boundary buffer zones.

3.1 *10-yr winter and summer mean fields*

Firstly, we analyze the distribution of 10-yr winter and summer mean precipitation rates. The GPCP (Global Precipitation Climatology Project) 1°×1° monthly precipitation data (Huffman et al., 1997) are used as observations. Figure 2 depicts the distribution of 10-yr winter and summer mean observed precipitation. It shows that winter precipitation (Fig.2a) is quite light on the East Asian Continent with 2 mm d^{-1} over the south of the Yangtze River, while heavy precipitation occurs over Japan, and oceanic regions of the east of Japan and Philippines. In summer (Fig.2c), there is heavy precipitation over the mainland of China, especially over South China where the precipitation rate is up to 8 mm d^{-1}, and heavy precipitation also occurs over the Bay of Bengal and Philippines. The MM5V3 also simulates the low winter mean precipitation over China, with 2 mm d^{-1} to the south of the Yangtze River, comparable with observations. And it simulates the high precipitation rates over Japan, and the east of Japan and Philippines, but it overestimates the precipitation rates in the east side of the Tibetan Plateau. The simulated distribution of 10-yr summer mean precipitation rates is consistent with observations. The model well simulates the high rates over the Bay of Bengal and South China. However, the model overestimates the precipitation over North China and in the east of Taiwan, and shifts the precipitation bands too east over South China. Figure 2 also shows the discrepancies between simulations and observations in winter and summer, respectively. In winter (Fig.2e), the differences are small over the Chinese Continent, except for the Yangtze-Huaihe River Basin and along the coastal regions of South China with the differences up to 1 mm d^{-1}. This indicates that the model can well simulate the distribution of

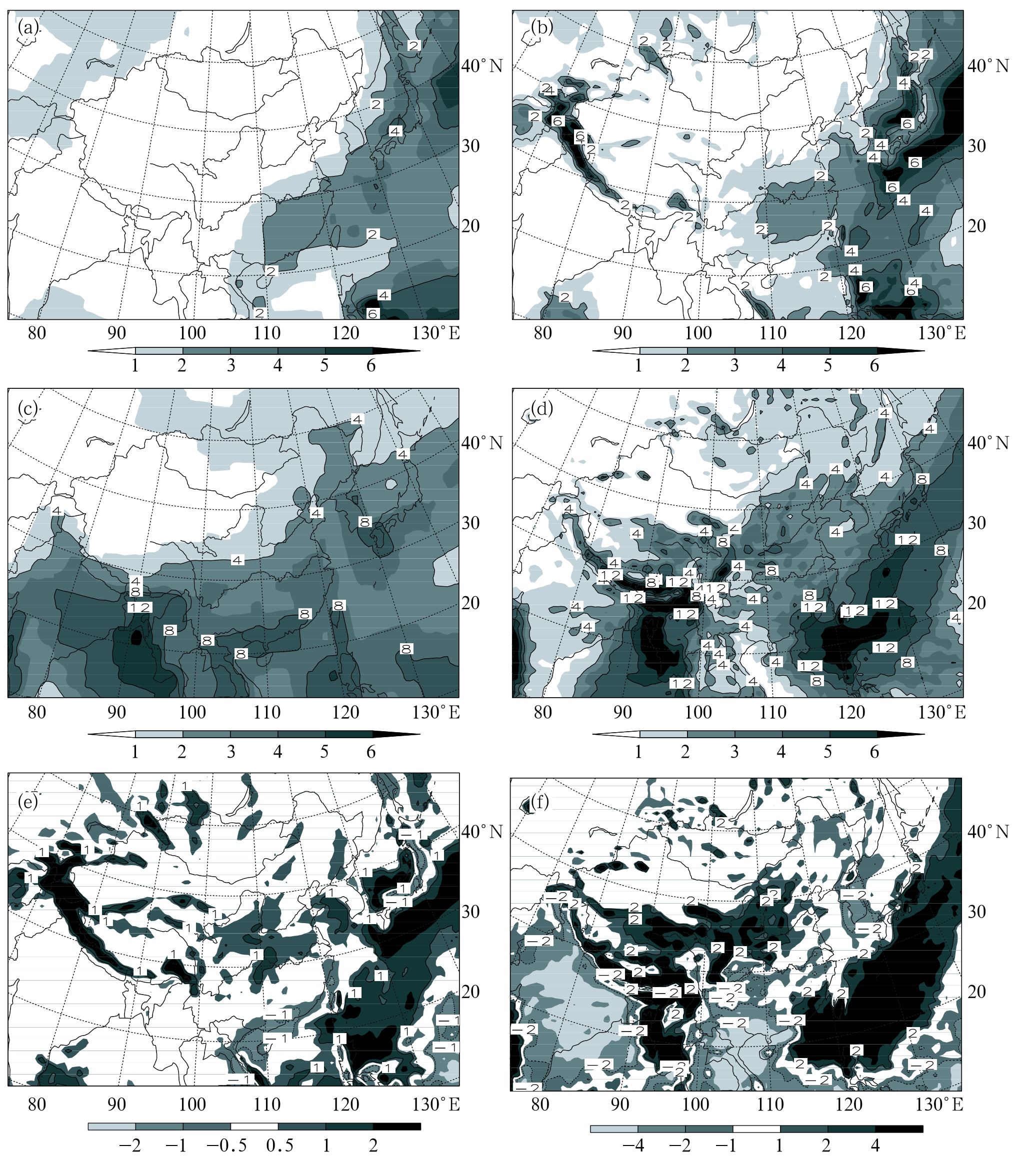

Fig.2. Winter and summer 10-yr mean precipitation rates (mm d^{-1}) based on observations (left panel) and simulations (right panel). (a) Winter, observation; (b) winter, simulation; (c) summer, observation; (d) summer, simulation; (e) winter, simulation minus observation; and (f) summer, simulation minus observation.

winter mean precipitation. In summer (Fig.2f), the model overestimates the precipitation rates more than 2 mm d^{-1} over the Hetao Plain of the Yellow River Basin and the coastal regions of the Southeast China, and underestimates the rates over Yunnan-Guizhou region and the Bay of Bengal. In both summer and winter, the model overestimates the precipitation rates over the oceanic region to the east of Taiwan, which may be due to a systematic error. In summary, the MM5V3 can well simulate the distribution of 10-yr mean precipitation, while it simulates precipitation in winter better than that in summer.

The NCEP/NCAR reanalyzed sea level pressure (SLP) is interpolated to the model domain as observations. Figure 3 depicts the simulated and observed 10-yr winter and summer mean SLP. In winter, the observed SLP (Fig.3a) is high in Mongolia, with the central pressure over 1032 hPa, whereas the distribution of the simulated SLP (Fig.3b) is comparable to reanalyses, with high value (over 1028 hPa in center) in Mongolia; however, the region of the simulated high SLP is too south. In summer, the 10-yr mean SLP is about 1008 hPa over the most Chinese continent for the NCEP/NCAR reanalysis dataset, with the high value region over the Tibetan Plateau, while the simulated pressure is comparable to it with 1008 hPa over the most region and high values over the plateau. In addition, by increasing resolution, the model can better simulate the depression over Sichuan in China associated with the southwest votex. To conclude, the MM5V3 can well simulate the distribution of 10-yr winter and summer mean SLP, and can capture SLP caused by topography and land-surface features in detail with the enhancement of resolution of the model.

Figure 4 depicts the 10-yr winter and summer mean 500 hPa geopotential height and temperature based on NCAR/NCEP reanalyses and regional simulation. In winter (Fig.4b), the distribution of the simulated 500 hPa circulation and temperature is comparable to observations, whereas the model well simulates the trough and its intensity over the coastal regions of the Northeast China. In summer (Fig.4d),

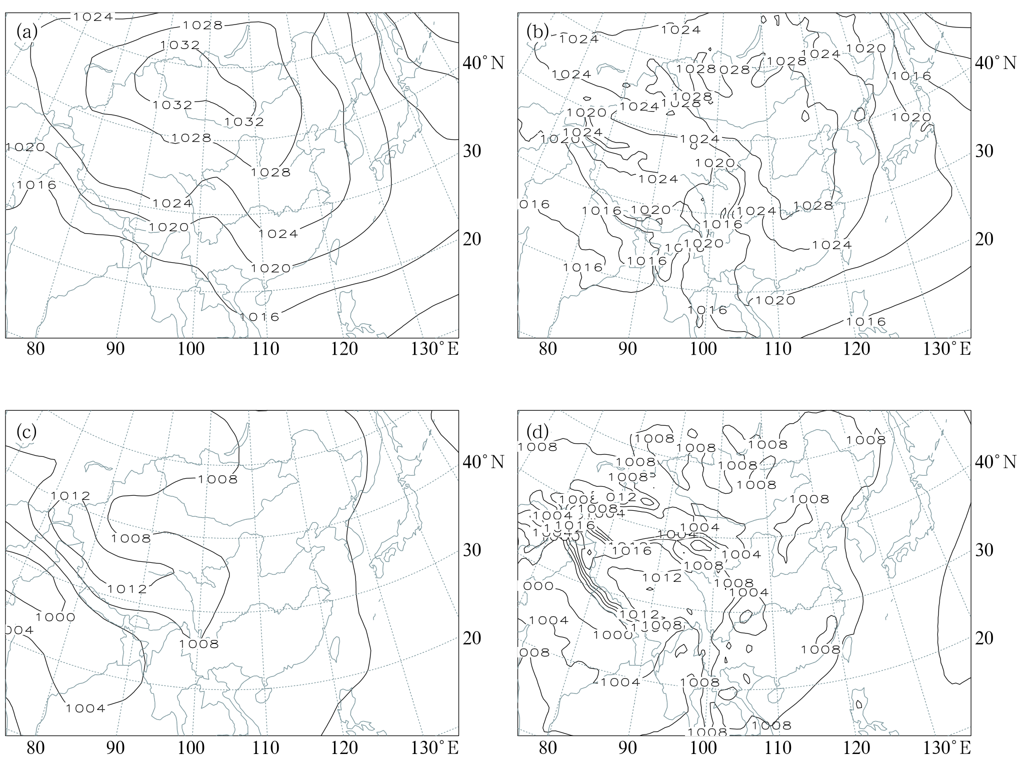

Fig.3. Winter and summer 10-yr mean sea level pressure (hPa) based on NCEP/NCAR reanalyses (left panel) and regional simulations (right panel). (a) Winter, reanalyses; (b) winter, simulation; (c) summer, reanalyses; and (d) summer, simulation.

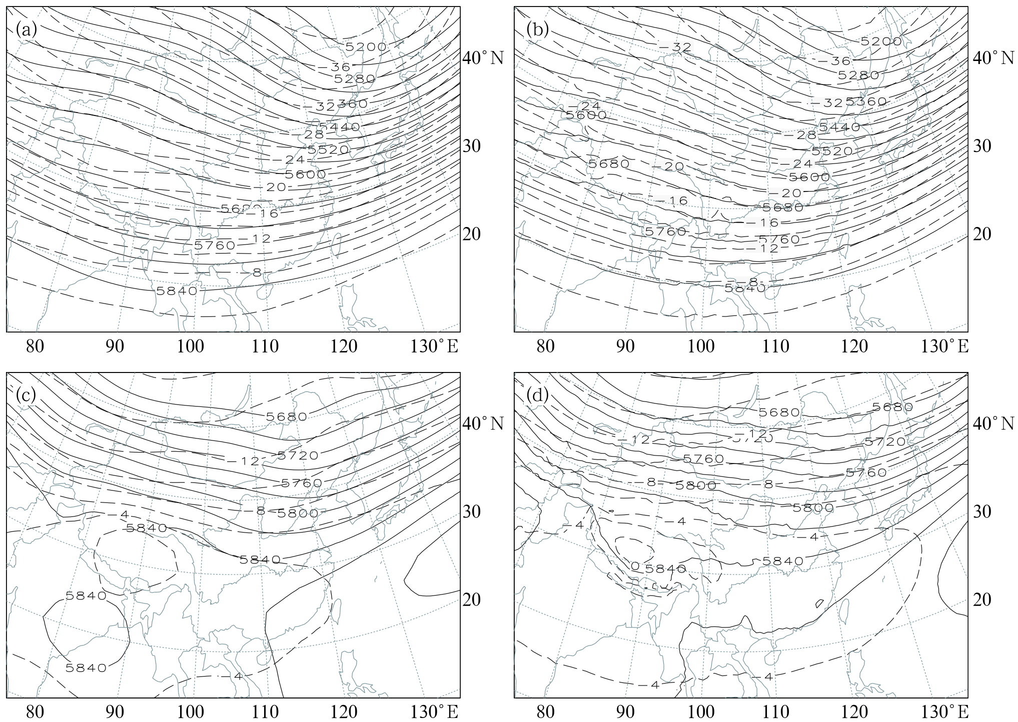

Fig.4. As in Fig.3, but for winter and summer 10-yr mean 500 hPa geopotential height (gpm) and temperature (°C).

the distribution of the simulated 500 hPa mean circulation and temperature shows good results in general. However, the model simulates the subtropical high too south and east. An underestimation is dominated over Northeast China, while an overestimation of the temperature is over North China. This may be due to the overestimation of summer precipitation over North China, which results in enlarging potential heat over the region, warm temperature of middle and low layers, and hence underestimation of trough.

Figure 5 demonstrates the 10-yr winter and summer mean 850 hPa winds and specific humidity based on NCEP/NCAR reanalyses and simulation. In winter, there are consistent west winds to the north of 20°N and east winds to the south of 20°N in both observations and simulations. Moisture is gathered mainly over the Bay of Bengal and South China Sea. In summer, in both observations and simulations, there are strong west and southwest winds in the north of the model region, which transfer moisture to South China and the Yangtze-Huaihe River Basin. Moisture source mainly exists over the Bay of Bengal based on observations, while simulation shows another moisture source over the South China Sea. The simulated 850 hPa specific humidity is higher than observations, which may cause the overestimation of the simulated summer precipitation.

The correlation coefficients of 10-yr winter and summer mean fields of the above mentioned variables between simulations and observations (Fig.5) indicate remarkable correlations ($\gamma_{0.01} = 0.244$) with largest coefficients (>0.6). In addition, such correlation coefficients in winter are larger than that in summer, which further reflects that the model's ability to simulate the regional climate change in winter is superior to that in summer.

From the above analysis, the MM5V3 can well simulate the mean circulation, temperature, as well as SLP, while the model simulates winter mean fields better than summer mean fields.

3.2 *Simulation of interannual variability*

The ability to simulate interannual variability is very important to examine the long-term simulation

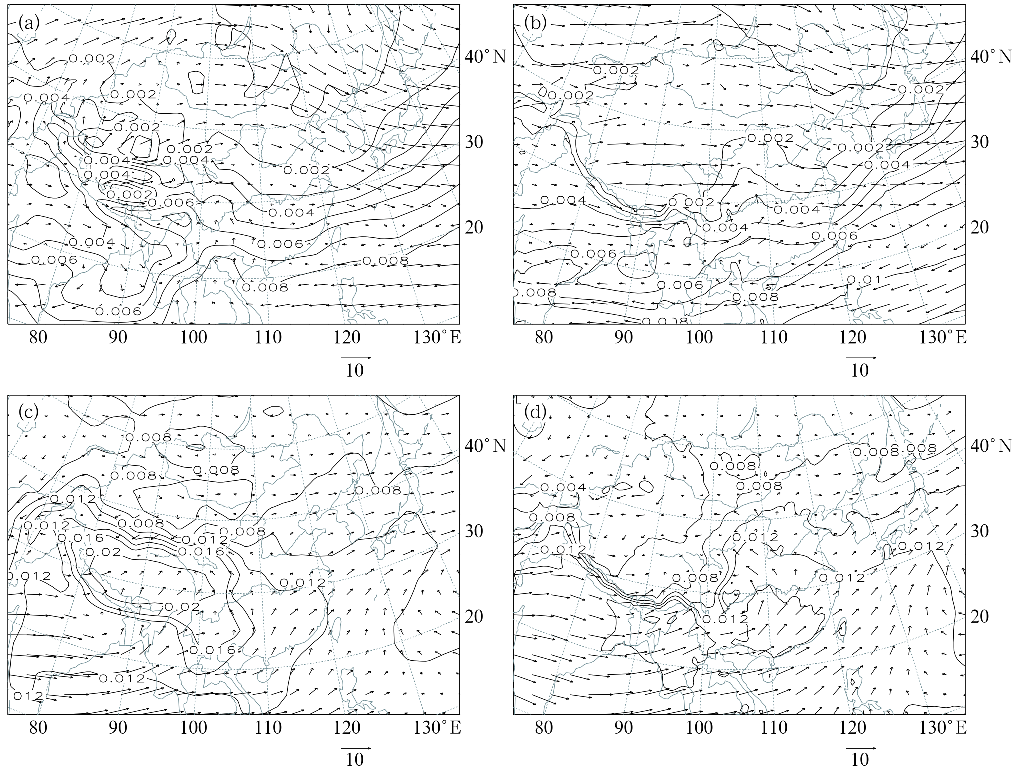

Fig.5. As in Fig.3, but for winter and summer 10-yr mean 850 hPa winds (m s^{-1}) and specific humidity (kg kg^{-1}).

Table 1. Correlation coefficients of precipitation, surface air temperature, 500 hPa height and temperature, 850 hPa wind and specific humidity between simulation and observation for winter and summer respectively during 1989-1998

	Precipitation	T_{sfc}	SLP	H_{500}	T_{500}	Q_{500}	U_{500}	V_{500}
Winter	0.80	0.98	0.93	0.99	0.99	0.93	0.90	0.48
Summer	0.64	0.93	0.78	0.99	0.98	0.48	0.81	0.81

of the regional climate. The CRU05 global 0.5°×0.5° surface air temperature data (Mark et al., 2000) and GPCP 1°×1° precipitation data are selected as observations. In general, the distribution of the simulated interannual variability is comparable to observations, with regards to the simulated and observed interannual variability on winter and summer mean surface air temperature (Fig.6). In winter, the observed interannual variability of surface air temperature is high in the north and low in the south. The highest variability is up to 2°C in the northwest of the model region and the lowest value exists mainly over the Yangtze-Huaihe River Valley and the area south of the valley. The simulated interannual variability of winter surface air temperature exhibits the similar pattern, but the model underestimates the high values in the northwest of model region, and overestimates the low value over the Yangtze-Huaihe River Valley and the area south of the valley. In summer, the interannual variability of surface air temperature is relatively low, generally varying between 0.4-0.8°C. The model overestimates temperature over Southwest China, Indo-China Peninsula as well as Northeast China (50°N), where the low center of the standard deviation of observations becomes to the high center but with very subtle difference about 0.4°C.

The simulated interannual variability of winter and summer mean precipitation rates is comparable

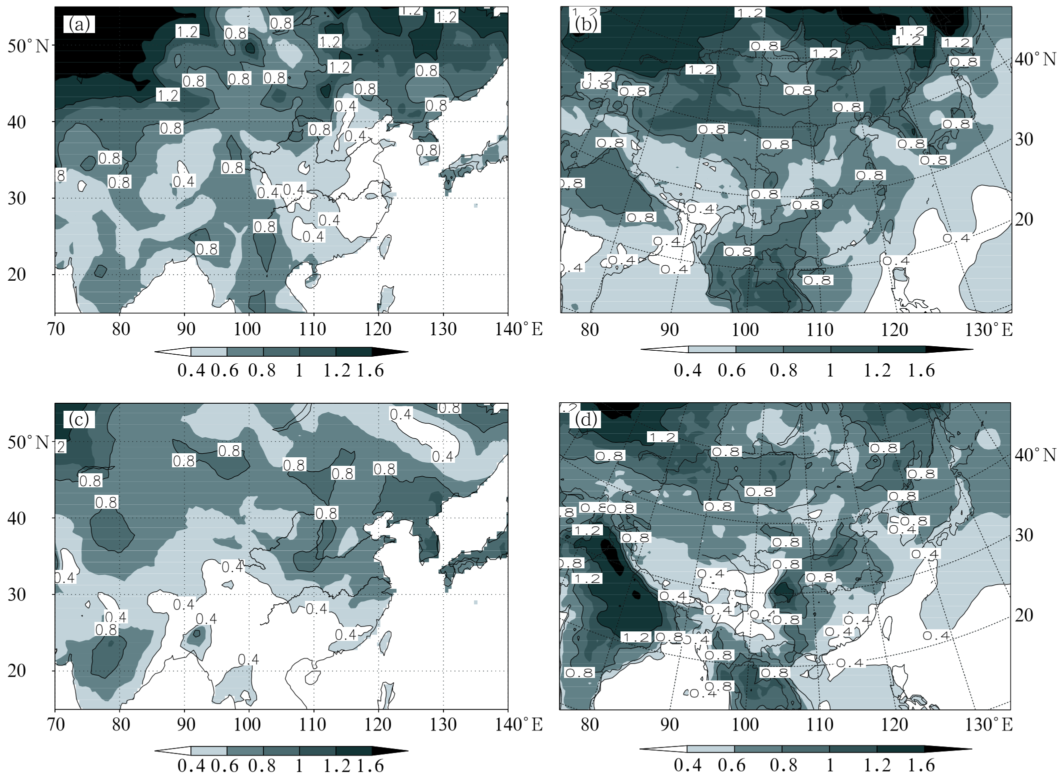

Fig.6. Standard deviations of winter and summer 10-yr mean surface air temperature (°C) based on CRU05 data (left panel) and regional simulation (right panel). (a) Winter, CRU05 data; (b) winter, simulation; (c) summer, CRU05 data; and (d) summer, simulation.

to observations (GPCP precipitation data) (Fig.7). In both simulations and observations, the variability of winter precipitation is large in the southeast of model region and low in other places. In summer, high values of the observed precipitation variability mainly appear over the Bay of Bengal and South China, which are captured by the MM5, except for the larger simulated variability than observations. Generally speaking, the model tends to overestimate the interannual variability of summer mean precipitation.

Figure 8 exhibits the anomalies of winter and summer mean precipitation over three sub-domains based on observations and simulations. The anomaly of simulated winter mean precipitation shows the consistent signs with observations over Northeast China, except that in 1994, and over North China except for 1992 and 1993, and the simulated values are close to the real ones except for 1990. Over South China, the simulated anomaly of winter precipitation is comparable to observations in both signs and magnitude in most years except for 1989, 1990, and 1993. On the other hand, the anomaly of summer mean precipitation is larger than that in winter. Over Northeast China, the anomaly of the simulated summer mean precipitation is consistent with observations except that from 1994 to 1996. The MM5V3 shows worse simulation of the anomaly of summer mean precipitation over North China, where the anomaly is overestimated and with reverse signs during almost half of these years. Such discrepancies may result from the overestimated precipitation rates over North China, hence, the ability of model to simulate the precipitation over the region is weak. For most of the years, the simulated anomaly of summer mean precipitation shows the same signs and close values to the observations. Overall, the model can well simulate the anomaly of winter mean precipitation over the three sub-domains, but less ability to simulate the summer anomaly in 1991, 1994, 1997, and 1998 when severe drought or flood occurred in some parts of China.

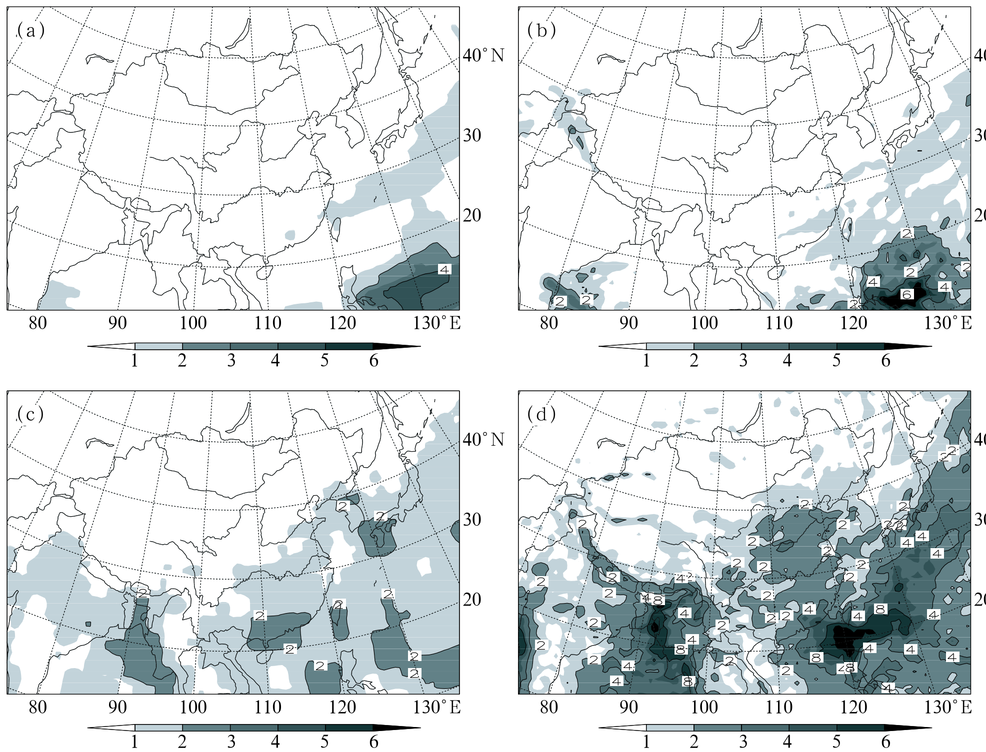

Fig.7. Standard deviations of winter and summer mean precipitation rates (mm d^{-1}) based on GPCP data (left panel) and regional simulation (right panel). (a) Winter, GPCP data; (b) winter, simulation; (c) summer, GPCP data; and (d) summer, simulation.

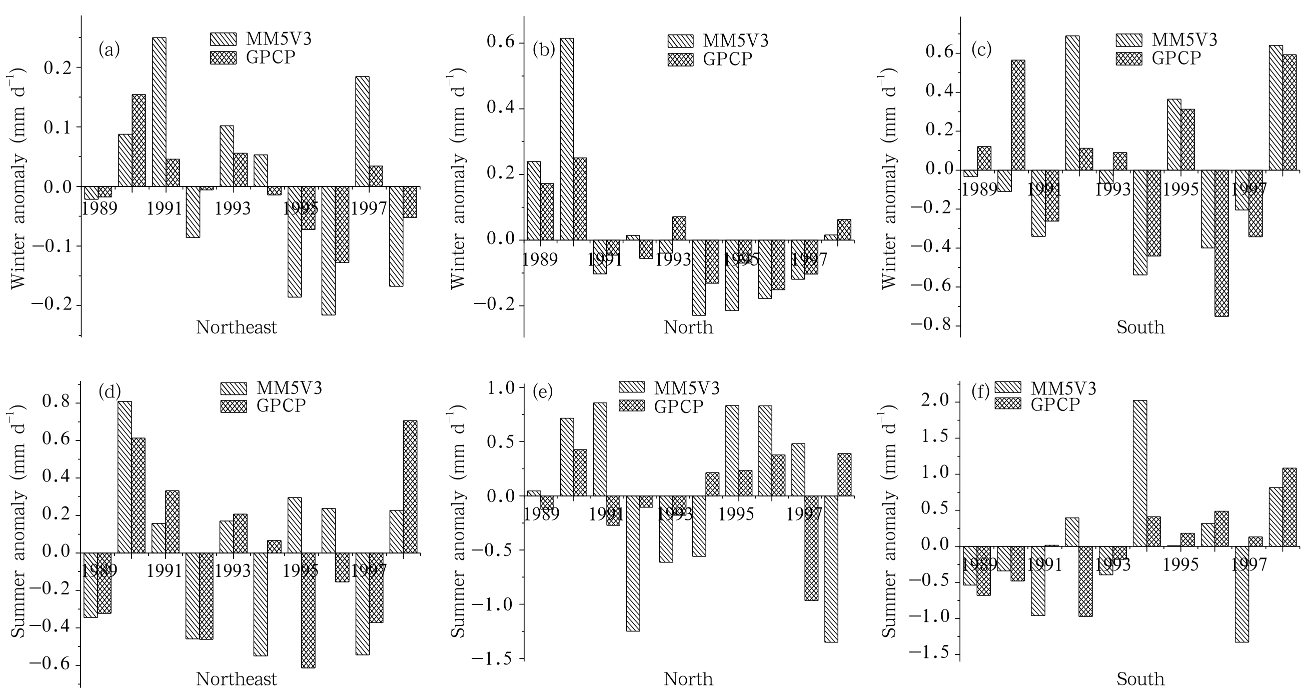

Fig.8. Anomalies of winter and summer mean precipitation rates (mm d^{-1}) in sub-domains based on observations and simulations. (a)(d) Northeast China; (b)(e) North China; and (c) (f) South China. The top three charts are for winter, and bottom three for summer.

With constrains of parameterization schemes and driven data, the ability of the regional model to capture the signal of extreme regional climate change is weak and needs to be improved.

The analysis of the anomaly of 10-yr winter and summer mean precipitation over three sub-domains indicates that the MM5V3 can generally simulate the interannual variation of winter and summer precipitation. The model's ability to simulate precipitation in winter is superior to summer. Additionally, the MM5V3 cannot well simulate the interannual variation of summer precipitation over North China.

Tables 2 and 3 list the anomaly correlation coefficients and root-mean-square (RMS) errors of 10-yr winter and summer mean geopotential height and temperature at 200 hPa and 500 hPa and SLP between the NCAR/NCEP reanalyses and simulations. Table 2 shows that all coefficients are relatively high (most of them over 0.75) and significantly pass through the critical value 0.244 with the confidence level of 0.01 in winter, while these coefficients are smaller in summer with some insignificant values. The results indicate that the ability of the model to simulate the climate in summer is inferior to that in winter. In addition, as shown in the tables, most of the anomaly correlation coefficients at 500 hPa are higher than that at 200 hPa, which indicates that the ability of the model to simulate the interannual variation of geopotential height and temperature at middle layers is better than that at high layers. The small values of these RMS errors in Table 3 suggest that the model can well simulate the seasonal mean features for all the years.

3.3 *Simulation of the El Niño years*

El Niño events evidently impact the monsoon and precipitation in East Asia. Of the 10 years of the simulation, there are three El Niño years, i.e., 1992, 1995, and 1998. In order to examine the ability of the

Table 2. Anomaly correlation coefficients of winter and summer mean geopotential height, temperature at 200 hPa and 500 hPa and sea level pressure (SLP) between observation and simulation

		1989	1990	1991	1992	1993	1994	1995	1996	1997	1998
Winter	H_{200}	0.912	0.978	0.855	0.938	0.916	0.884	0.958	0.836	0.806	0.688
	T_{200}	0.936	0.762	0.798	0.767	0.866	0.727	0.919	0.791	0.834	0.904
	H_{500}	0.969	0.955	0.929	0.923	0.887	0.949	0.976	0.971	0.927	0.842
	T_{500}	0.866	0.934	0.861	0.934	0.915	0.876	0.915	0.875	0.868	0.661
	SLP	0.885	0.959	0.846	0.923	0.734	0.874	0.786	0.971	0.819	0.782
Summer	H_{200}	0.795	0.637	0.716	0.854	0.837	0.247	0.822	0.201	0.530	0.635
	T_{200}	0.159	0.416	0.091	0.529	0.326	0.688	0.563	0.678	0.720	0.567
	H_{500}	0.847	0.675	0.848	0.784	0.860	0.354	0.783	0.355	0.621	0.649
	T_{500}	0.709	0.621	0.627	0.806	0.646	0.397	0.685	-0.01	0.539	0.702
	SLP	0.908	0.385	0.496	0.343	0.669	-0.04	0.829	0.154	0.629	0.437

Table 3. Root-mean-square errors of winter and summer mean geopotential height, temperature at 200 hPa and 500 hPa and sea level pressure (SLP) between observation and simulation (height: 10 gpm, temperature: °C, SLP: hPa)

		1989	1990	1991	1992	1993	1994	1995	1996	1997	1998
Winter	H_{200}	4.09	3.44	4.39	2.98	2.61	4.20	4.08	3.85	4.51	4.75
	T_{200}	1.19	1.05	1.62	0.99	1.11	1.57	1.51	1.17	1.44	1.77
	H_{500}	1.15	1.06	1.26	1.25	1.25	1.23	1.22	1.13	1.19	1.76
	T_{500}	0.93	0.56	0.89	0.49	0.53	0.98	0.65	0.70	0.77	0.74
	SLP	2.26	2.36	2.48	2.52	2.46	2.54	2.71	2.46	2.54	2.93
Summer	H_{200}	4.53	4.44	4.34	4.01	4.91	2.95	4.49	3.43	3.66	5.85
	T_{200}	2.26	2.66	2.53	2.68	3.26	2.91	2.96	2.50	2.38	2.65
	H_{500}	1.09	1.31	1.04	1.00	0.88	2.32	1.41	0.96	1.08	1.51
	T_{500}	1.15	0.89	1.00	0.88	1.10	0.82	1.00	0.86	0.92	1.29
	SLP	1.96	2.10	2.28	2.20	2.04	2.41	2.82	2.37	2.39	2.21

MM5V3 to simulate the short-term regional climate change caused by El Niño events, the simulation of the precipitation anomaly in the three El Niño years has been analyzed. The simulated anomaly of winter mean precipitation rates is comparable to observations, but the model shows the different ability to simulate the summer mean precipitation rates in the three El Niño years. The results exhibit variability for the anomaly of summer precipitation rates in the three El Niño years. In 1992, the model well simulated the negative precipitation anomaly in the most regions along the Yangtze-Huaihe River Basin, Northeast China, Japan, and the coastal areas of South China, and relatively well simulated the negative precipitation anomaly over the Tibetan Plateau and the southwest of the region, but the simulated precipitation anomaly over the Hetao Plain and the regions south of the Yangtze River had the reverse signs compared with observations. In 1995, the model simulated the distribution of the precipitation anomaly in general, and the simulated negative precipitation anomaly along the Yangtze-Huaihe River Basin, Northeast China, as well as the west

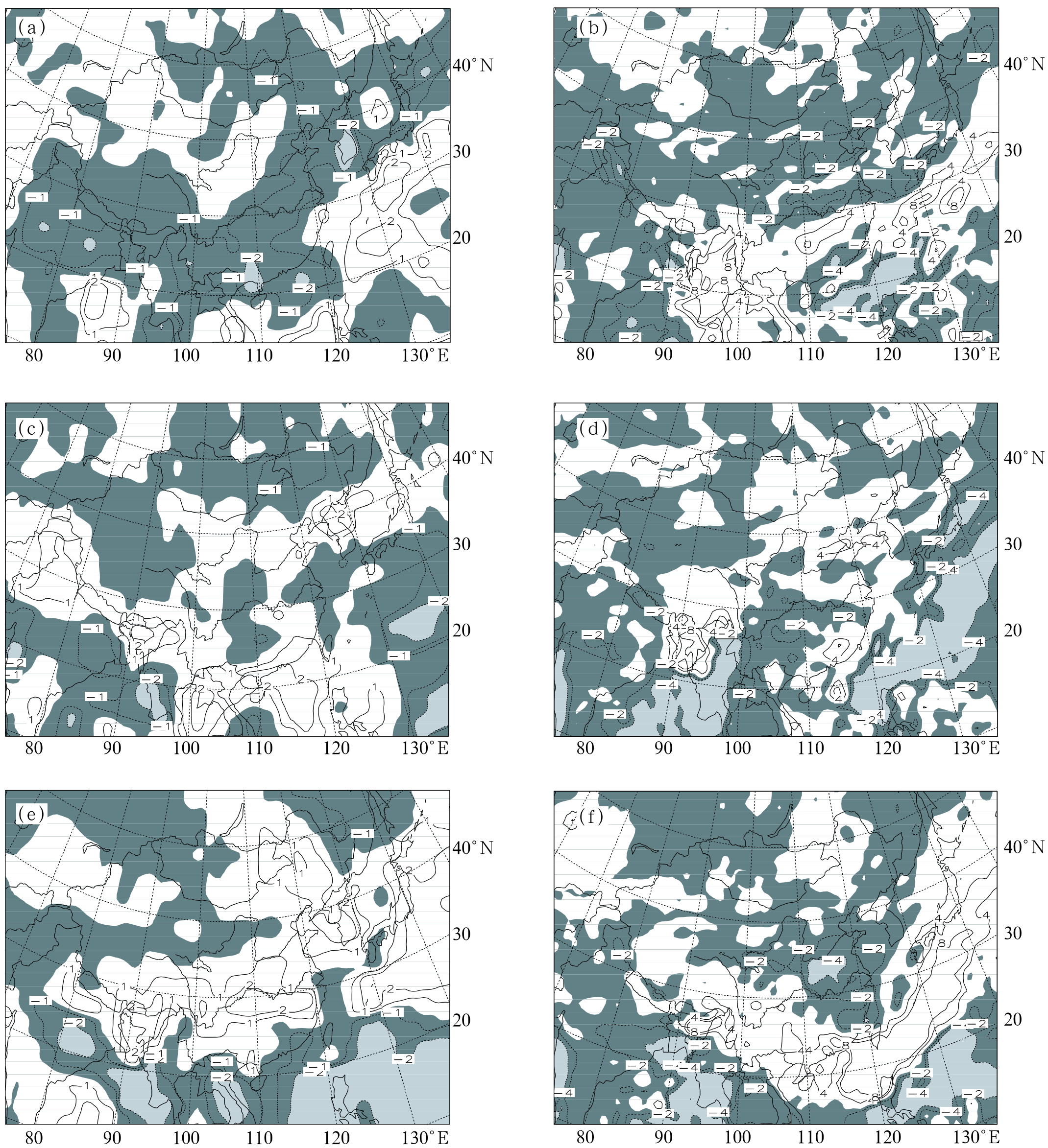

Fig.9. Anomaly of summer mean precipitation rates (mm d^{-1}) in the three El Niño years based on GPCP data (left panel) and regional simulation (right panel) (top: 1992, middle: 1995, bottom: 1998).

Tarim Basin was consistent with observations, and positive precipitation anomalies over the Korea Peninsula and the coastal areas of South China were relatively well simulated, though the positive precipitation anomaly over the South China Sea was not well simulated. In 1998, the observed precipitation anomaly over most regions from the south of the Yangtze River to the Korea Peninsula and Northeast China was positive, and the anomaly along the costal South China was negative, while the simulated precipitation anomaly had the reverse signs to observations in these places, and the positive precipitation anomaly was overestimated over the ocean east of Taiwan Province of China. Generally speaking, the model well simulates the anomaly of summer mean precipitation in 1992 and 1995, but has not simulated that in 1998. This indicates that the MM5V3 has the ability to simulate strong climate change signals to some extent, but it needs advanced improvements.

4. Conclusions

The paper utilized the NCAR MM5V3 to perform a 10-yr integration in East Asia, and compared the simulated winter and summer mean results with observations. The main conclusions can be drawn as follows.

(1) The model could well simulate the 10-yr winter and summer mean circulation, temperature, and sea level pressure. Meantime, the model could well simulate the distribution and intensity of winter mean precipitation rates. It also simulated the distribution of summer mean precipitation rates, while it overestimated the summer mean precipitation over North China. With respect to the results of circulation, temperature or precipitation, the model generally can simulate 10-yr seasonal mean fields.

(2) The model could simulate the interannual variation of seasonal precipitation and surface air temperature, and the simulated anomalies of seasonal mean precipitation over different sub-domains showed the same tentency as observations in most years. The model could simulate mean circulation at middle and high layers in winter, which was not well simulated in summer. Nevertheless, the MM5V3 could simulate the interannual variation of the regional climate.

(3) The model demonstrated the different ability to simulate the regional climate change associated with the El Nino events. It well simulated the anomaly of summer mean precipitation in 1992 and 1995, but could not simulate that in 1998.

(4) Based on the overall performance of the simulation experiments, the MM5V3 simulated winter climate superior to summer climate.

In a word, the MM5V3 has the ability to simulate the regional climate change, and can be used for long-term regional climate simulation, although its physical processes need to be further improved and investigated.

REFERENCES

Chen Fei and Jimy Dudhia, 2001a: Coupling an advanced land surface-hydrology model with the Penn State-NCAR MM5 modeling system. Part I : Model implementation and sensitivity. *Mon. Wea. Rev.*, **129**(4), 569-585.

Chen Fei and Jimy Dudhia, 2001b: Coupling an advanced land surface-hydrology model with the Penn State-NCAR MM5 modeling system. Part II : Preliminary model validation. *Mon. Wea. Rev.*, **129**(4), 587-604.

Chen Ming and Fu Congbin, 2000: A nested procedure between regional and global climate model and its application in long term climate simulations. *Chinese J. Atmos. Sci.,* **24**(2), 253-262.

Crawford, Todd M., David J. Stensrud, Franz Mora et al., 2001: Value of incorporating satellite-derived land cover data in MM5/place for simulating surface temperature. *J. Hydrometeorology*, **2**(5), 453-468.

Dudhia, Jimuy, Dave Gill, Yong-Run Guo, Kevin Manning et al., 2001: PSU/NCAR mesoscale modeling system tutorial class notes and users' guide (MM5 modeling system version 3), NCAR/MMM.

Girogi, Filippo, Maria Rosaria Marinucci, and Gary T. Bates, 1993a: Development of a second-generation regional climate model (RegCM2). Part I: Boundary-layer and radiative transfer processes. *Mon. Wea. Rev.*, **121**(10), 2794-2813.

Girogi, Filippo, Maria Rosaria Marinucci, Gary T. Bates et al., 1993b: Development of a second-generation regional climate model (RegCM2). Part II : Convective processes and assimilation of lateral boundary conditions. *Mon. Wea. Rev.*, **121**(10), 2814-2822.

Huffman, George J., Robert F. Adler, Philip Arkin, Alfred Chang et al., 1997: The global precipitation climatology project (GPCP) combined precipitation data set. *Bull. Amer. Soc.*, **78**(1), 5-20.

Jiang Yong, Zhao Ming, Tang Jianping, and Su Bingkai, 2002: Application of a new boundary layer parameterization scheme in MM5 and comparison of different boundary layer parameterization. *Scientia Meteorologica Sinica*, **22**(3), 253-263. (in Chinese)

Kalnay E., M. Kanamitsu, R. Kistler, W. Collins et al., 1996: The NCEP/NCAR 40-year reanalysis project. *Bull. Amer. Meteor. Soc.*, **779**(3), 437-471.

Lee Dong-Kyou and Myoung-Seak Suh, 2000: Ten-year East Asian summer monsoon simulation using a regional climate model (RegCM2). *J. Geophys. Res.*, **105**(D24), 29565-29577.

Leung L. Ruby, Qian Yun, and Bian Xindi, 2003a: Hydroclimate of the western United States based on observations and regional climate simulation of 1981-2000. Part I: Seasonal statistics. *J. Climate*, **16**(12), 1892-1911.

Leung L. Ruby, Qian Yun, Bian Xindi, and Allen Hunt, 2003b: Hydroclimate of the western United States based on observations and regional climate simulation of 1981-2000. Part II: Mesoscale ENSO anomalies. *J. Climate*, **16**(12), 1912-1928.

Liang Xinzhong, Kunkel Kenneth E,, and Samel Arthur N., 2001: Development of a regional climate model for U.S. midwest application. Part I: Sensitivity to buffer zone treatment. *J. Climate*, **14** (23), 4363-4378.

Liu Dong, 2003: Performance verification of mesoscale model MM5V3 to regional climate simulation. *Plateau Meteorology*, **22**(1), 71-77. (in Chinese)

Liu Yiming and Ding Yihui, 2001: Modified mass flux cumulus parameterization scheme and its simulation experiment. Part I: Mass flux scheme and its simulation of the flooding in 1991. *Acta Meteorologica Sinica*, **59**(1), 10-22. (in Chinese)

Liu Yongqiang, Avissar Roni, and Giorgi Filippo, 1996: Simulation with the regional climate model RegCM2 of extremely anomalous precipitation during the 1991 East Asian flood: An evaluation study. *J. Geophys. Res.*, **101**(D21), 26199-26215.

Luo Yong and Zhao Zongci, 1997: Numerical simulation of East Asian regional climate with NCAR RegCM2. *Quarterly Journal of Applied Meteorology*, **8**(Suppl), 124-133. (in Chinese)

Luo Yong, Zhao Zongci, and Ding Yihui, 2002: Ability of NCAR RegCM2 in reproducing the dominant physical processes during the anomalous rainfall episodes in the summer of 1991 over the Yangtze-Huaihe valley. *Advances in Atmospheric Sciences*, **19**(2), 236-254.

Mark, New, Hulme Mike, and Jones Phil, 2000: Representing twentieth-century space-time climate variability. Part II: Development of 1901-1996 monthly grids of terrestrial surface climate. *J. Climate*, **13**(13), 2217-2238.

Shi Xueli, Ding Yihui, and Liu Yiming, 2001: Simulation experiments of summer rainbelt in China with the regional climate model. *Climatic and Enviromental Research*, **6**(2), 249-254.

Su Bingkai, Tang Jianping, Zhong Zhong et al., 2002: A research on high performance simulator for disaster weather and climate. *J. Nanjing University (Natural Sciences)*, **38**(3), 366-375.

Wang Shourong, Huang Ronghui, Ding Yihui, Ruby L. Leung et al., 2002: Numerical simulation experiments by nesting hydrology model DHSVM with regional climate model RegCM2/China. *Acta Meteorologica Sinica*, **60**(4), 421-427. (in Chinese)

Wei Helin, William J. Gutowski, Charles J. Vorosmarty, and Balazs M. Fekete, 2002: Calibration and validation of a regional climate model for Pan-Arctic hydrologic simulation. *J. Climate*, **15**(22), 3222-3236.

Xiong Zhe, 2001: Simulation and analysis of intra-annual climate variance using regional climate model in East Asia. Doctoral Dissertation, Institute of Atmospheric Physics, Chinese Academy of Sciences. (in Chinese)

Zhao Zongci and Luo Yong, 1998: Advances in regional climate modeling since 1990. *Acta Meteorologica Sinica*, **56**(2), 225-246. (in Chinese)

Zhao Zongci and Luo Yong, 1999: Investigations of application for the regional climate model over East Asia. *Chinese J. Atmos. Sci.*, **23**(5), 522-532.